Percolation strategy to improve the production of plants with high pathogen susceptibility

J. E. Ramírez,[1,2,*] E. Molina-Gayosso,[3,†] J. Lozada-Lechuga,[3] L. M. Flores-Rojas,[3] M. I. Martínez,[1] and A. Fernández Téllez[1]

[1]*Facultad de Ciencias Físico Matemáticas, Benemérita Universidad Autónoma de Puebla, Apartado Postal 165, 72000 Puebla, Pue., México*
[2]*Departamento de Física de Partículas, Universidad de Santiago de Compostela, E-15782 Santiago de Compostela, España*
[3]*Universidad Politécnica de Puebla, Tercer carril del Ejido Serrano, 72640, Juan C. Bonilla, Pue., México*

We use percolation theory to propose a strategy that increases the production yield of plants with high susceptibility to a pathogen plague. This strategy consists in sowing a second variety with a lower susceptibility. The percolation threshold is determined as a function of the plant density, the mixture of plants, the pathogen susceptibilities, and the initial percentage of inoculated soil. Moreover, we provide conditions to prevent the formation of a spanning cluster of infected plants. We present an application of this strategy to a particular chili plantation. Under controlled conditions, we measure the pathogen susceptibilities to different strains of *Phytophthora capsici* for three varieties of chili peppers with high commercial value in Mexico. Then we simulate the propagation process of the pathogen on nearest and next-to-nearest-neighbor square lattices. We find that the production yield of plantations with the highest susceptibility can be significantly increased as a result of this novel application of percolation theory.

I. INTRODUCTION

Percolation theory is a branch of statistical physics that addresses transport phenomena in porous media [1,2]. It explains, for instance, the conditions under which filtration of water through a wall or how the current flow goes through an electrical mesh can occur [3–6]. The basic idea in percolation theory is to represent porous media as a lattice whose sites either permit the flow (and then are said to be *occupied*) or not. Each site has a probability p (independent of the neighboring sites) of being designated as occupied or, equivalently, a probability $1 - p$ of being designated as *empty* [4]. Evidently the value of p determines if the transport phenomenon takes place or not. If p is too small, then there are too few occupied sites and the transport process cannot occur. Contrarily, if p takes on a value close to 1, then there are plenty of occupied places and one expects transport to occur [4–8]. The case of interest is that in which the number of occupied sites is just enough to allow the transport phenomenon to happen. In such a situation, there is a critical value p_c, called the *percolation threshold*, that bounds from below the values of p for which the transport phenomena will occur. Its determination is one of the fundamental problems in percolation theory [6]. Since finding the percolation threshold analytically is not possible in most applications, computational methods have proved to be an effective alternative [4,6–8].

Percolation theory has been applied in a wide variety of situations, ranging from the study of the formation of galactic structures [9–11] to super-cooled water [12,13],

fragmentation [14–16], porous materials [2,17,18], earthquakes [19–21], forest fires [22–24], deforestation [25], and the properties of the quark-gluon plasma [26–28].

An application of particular interest is the propagation of diseases where a susceptible-infected-recovered (SIR) model is used to determine the critical number of edges that would prevent the propagation of the disease in a certain population [29–37]. In particular, disease propagation models for plants have been proposed in Refs. [38–43] in which different media are considered for pathogen transport, like thin films of water or air.

The interest in applying models like the one described above is due to the great threat that plagues of insects or gastropods, on one hand, and the spread of diseases caused by bacteria, fungi, and oomycetes, on the other, pose on the production of vegetables. The effects range from a reduced production to the complete loss of a plantation or even the transmission of the agent to other plantations sharing the irrigation system, for example. The associated economic losses render the study of the propagation of disease agents and its eventual control necessary.

In the taxonomic class of oomycetes we find the organisms that cause epiphytic interactions with the most destructive effects on crops: the genus *Phytophthora* (from Greek, meaning literally *phyto*, "plant," and *phthora*, "destroyer" [44]) [45,46]. Long considered as lower fungi, these organisms are more closely related to brown algae and green plants [47,48]. However, they share morphological characteristics with true fungi (Eumycota), such as mycelial growth and the dispersion of spores of mitotic or asexual origin. The latter have a distinctive feature that causes them to have a great impact on the plant kingdom as phytopathogens: their movement by means of flagella [49,50].

These biflagellate zoospores have a mastigoneous flagellum with microfibrils that serve to assist or guide

---

*Corresponding author for topics related to the model and the simulations. jerc.fis@gmail.com

†Corresponding author for topics related to experimental results. eduardo.molina@uppuebla.edu.mx

movement. They can disperse through water films or soil moisture, including those on the surface of plants. These zoospores emerge from mature sporangia in quantities of 20 to 40 motile zoospores, which swim chemotactically toward the plants [49,51,52].

When the zoospores reach the surface of the roots, they lose their flagella, encyst in the host, and form a germination tube through which they penetrate the surface of the plant [53,54]. However, many species of *Phytophthora* can persist as sapro-phytes if the environmental conditions are not appropriate but become parasitic in the presence of susceptible hosts [46,52].

Damages produced by the species of the genus *Phytoph-thora* include rotting in seedlings, tubers, corms, the base of the stem and other organs, staying mainly at the root of many plant species [55]. The variation in infection caused by the different species of *Phytophthora* is associated with the environment conditions, which usually include optimal temperature and humidity, exhibiting a transition of rapid propagation in edaphic media of high humidity. Irrigation is then considered one of the most important means of dissemi-nation since it facilitates the spreading of zoospores [49,56].

Due to the physiology of the oomycetes, most of the fungicides have no effect on them. Therefore, research on non-chemical strategies that minimize or eliminate the propagation of the pathogen is necessary.

In this work we model the propagation of the pathogen *Phytophthora* as a transport phenomenon over a plantation. As happens with some diseases, certain varieties of plants have an intrinsic tolerance to *Phytophthora* [57]. These can inhibit the spread of the pathogen and therefore may be used as protective barriers for plants with less resistance. We incorporate this idea into our model, considering plantations comprising a mixture of varieties with high and low tolerance to the pathogen. Since it is *a priori* unknown whether one particular seed of a given variety will yield a nontolerant plant, we assume the latter are uniformly distributed over the plantation.

We use percolation theory to propose a strategy that sup-presses or at least minimizes the spread of *Phytophthora capsici* in chili plantations. We are interested in predicting the conditions on the parameters of the crops that reduce the propagation of the disease and maximize the total plant pro-duction. To this end, we model plantations as square matrices with a plant in each of their cells.

We report the pathogen susceptibility for three varieties of chili plants. With these data we are able to find a way to pre-vent the disease from propagating over the whole plantation for the most susceptible chili variety. By mixing with a second chili variety, our model yields the mixing proportion and the plant density for a given initial percentage of inoculated soil that would contain and prevent the pathogen from spreading.

This paper is organized as follows. In Sec. II, we describe the model for pathogen propagation over a plantation in terms of percolation theory. Then we find the percolation threshold for these systems implemented in regular lattices as a function of the mixing proportion, the pathogen susceptibilities, and the initial percentage of inoculated soil. Section III describes the experimental setup for the determination of the pathogen susceptibility of four varieties of *Phytophthora* for three commercially relevant varieties of chili: "Arbol," "Serrano,"

TABLE I. Percolation threshold for different regular lattices. Data taken from Ref. [4].

Lattice	p_c
2N square	0.592...
3N square	0.407...
Triangular	0.5
Hexagonal	0.697...

and "Poblano." In Sec. IV we report the susceptibility mea-surements and obtain the mixing thresholds for which the disease will only propagate over finite clusters even if all cells in the plantation are sowed. In addition, for the case of high susceptibility measured for the "Arbol" variety when exposed to *P. capsici*, we determine by computer simulation the total production yield as a function of the occupation probability and the mixing proportion with a second chili variety of lower susceptibility. A discussion and a comparison with the alternate rows sowing strategy is included in Sec. V. Section VI contains the conclusions of this work.

II. MODEL

The basic percolation model studies the formation of clusters on regular lattices with N sites, where each site is available to the process with a probability p. It is of particular interest to determine the percolation threshold p_c, that is, the minimum probability at which a spanning cluster extending across the percolating system appears. This critical density depends on the properties of the lattice, as illustrated in Table I. There we show the percolation threshold for the near-est (denoted by 2N) and next-to-nearest-neighbor (denoted by 3N) square, triangular, and hexagonal lattices.

A. Percolation threshold

In this work the sites in the lattice represent plants of two different varieties growing on specific soil. Each variety has a particular pathogen susceptibility, which is the probability of being infected by a specific pathogen. We denote by A and B the different plant varieties in the plantation, while χ_A and χ_B denote their pathogen susceptibilities.

We consider a regular lattice with a probability of occupa-tion p. The available sites in the lattice can be occupied by two different types of plants, distributed in a homogeneous way according to a certain proportion. We define M as the probability that an available site is occupied by a plant of variety A, so $(1 - M)$ it is the probability that an available site is occupied by a plant of variety B. We are interested in studying the spread of the disease on plants which can get infected. Because the pathogen susceptibilities may be different from one, then the spread of the disease occurs on a percolating system with an effective probability p_{eff} that depends explicitly on p, χ_A, χ_B, and M.

In a percolating system with given p, χ_A, χ_B, and M, the average number of effective sites available for the spread of the disease can be written as $N_{\text{dis}} = \langle N_A \rangle + \langle N_B \rangle$, where

$\langle N_{A,B} \rangle$ is the average number of susceptible sites of type A or B, which can be calculated as

$$\langle N_A \rangle = NM\chi_A p; \tag{1}$$

$$\langle N_B \rangle = N(1-M)\chi_B p. \tag{2}$$

In addition to the average number of plants that can get infected, it is necessary to take into account the fraction of cells that are inoculated with the pathogen. These can be located in occupied sites or in plants that are resistant. Even in these cases, the pathogen may spread to neighboring plants. Defining I as the probability that a cell in the lattice is inoculated, we have that the average number $\mathcal{N}$ of cells through which the propagation process can occur is

$$\mathcal{N} = Np_{\text{eff}} = N_{\text{dis}} + (N - N_{\text{dis}})I, \tag{3}$$

where the second term on the right-hand side has been added to consider the inoculated sites that match the situation described above. This last equation corresponds to a percolation process that occurs on a lattice with an effective probability given by

$$p_{\text{eff}} = I + (1-I)[M\chi_A + (1-M)\chi_B]p. \tag{4}$$

Equation (4) is crucial, since it determines the formation properties of clusters of plants that have been infected by the pathogen, including those plants that do not manifest the disease but can propagate it. The existence of the spanning cluster of infected plants occurs when the value of p_{eff} in Eq. (4) coincides with that of the percolation threshold of the lattice. In that case, the percolation threshold of the system is given by

$$p_c^* = \frac{p_c - I}{(1-I)[M\chi_A + (1-M)\chi_B]}. \tag{5}$$

In general, there is not a direct way to compare p_c^* to p_c. However, it is possible to determine specific conditions for which a spanning cluster will not exist. If we consider that p_c^* can only take values between zero and one, then the no percolation condition for the values of I, M, χ_A, and χ_B is $(1-I)[M\chi_A + (1-M)\chi_B] \leqslant p_c - I$. This is an important condition because once knowing the pathogen susceptibilities of the plants, we can determine the proportion M that guarantees that no percolating cluster is formed, despite a fraction I of soil area might be inoculated.

B. Disease incidence

Another important parameter that can be calculated is the extent of disease incidence on the sown plants. Note that independently of the lattice, the pathogen can spread on plants that are susceptible and belong to the same cluster.

Because some pathogens can present latency stages when they are in an adverse environment, any point in the lattice can be the source of infection, even a place with no plant or with a plant resistant to the pathogen. This fact highly complicates the determination of an analytical result for the percentage of the plantation that can be damaged by the spread of the disease. If the initial point of infection is an empty place or a place occupied by a plant resistant to the pathogen, then the disease can be transmitted to more than
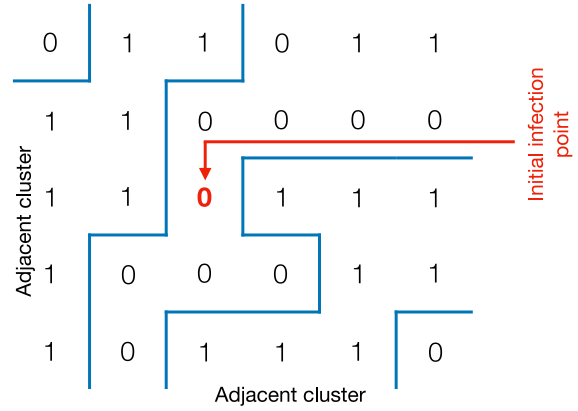

FIG. 1. Example of an initially infected point (red zero) surrounded by two adjacent and disjoint clusters delimited by a blue line for a nearest-neighbor square lattice with $p = 0.6$.

one adjacent cluster as shown in Fig. 1, where an initial point of infection allows the pathogen to spread over two disjoint clusters. For this reason we expect the average number of cells where the pathogen causes damage to be slightly larger than the average cluster size, for $p_{\text{eff}} \sim p_c$, as a result of the connecting effect between disjoint clusters by the initial infection point. On the other hand, for $p_{\text{eff}} < p_c$, we expected that the contribution of the initial point of infection be through finite clusters or isolated sites. Finally, for $p_{\text{eff}} > p_c$, the initial point of infection belongs to the spanning cluster as p_{eff} takes values greater than the percolation threshold. Consequently, if there is more than one initial point of infection in the system, we expect the appearance of cells connecting two adjacent disjoint clusters to magnify. Evidently, this effect does not scale linearly, since it may happen that two initial points transmit the disease to the same cluster. In Sec. IV we will discuss the implications of considering several initial points.

Finally, if we know the pathogen susceptibilities χ_A and χ_B of two varieties, then we can predict the mixture of seeds and the fraction of sown cells that will maximize the total yield obtained from the whole production of A and B, which may be computed as the number of cells for which the pathogen could not spread.

C. Simulation on square lattices

Traditionally, crops are planted in parallel rows on the soil, so that the seeds are sown in a square lattice-type arrangement. The best approximation to represent the system is a Boolean matrix whose values on each entry depend on whether seed is deposited or not in the cell. The cells are spaced according to the maximum displacement length that the pathogen can travel. We do not know *a priori* what value corresponds to a given cell (this is, we do not know whether a seed was sown there). Therefore, we assign a 1 to each entry in the matrix according to the occupation probability p. Given a proportion mixture $0 < M < 1$, we assign randomly to each occupied cell (i.e., to each entry in the matrix with a value of 1) a plant variety A or B. Specifically, we generate for each cell a random number x between zero and one and define that, if $x < M$, then a plant of variety A has been sown. Otherwise, it

(a)

1	1	1	0	1
1	0	1	1	1
1	1	1	0	0
0	1	1	1	1
0	1	0	1	1

(b)

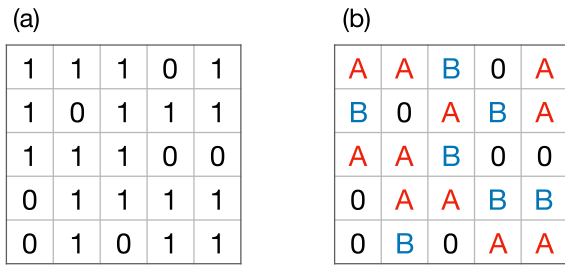| A | A | B | 0 | A |
B	0	A	B	A
A	A	B	0	0
0	A	A	B	B
0	B	0	A	A

FIG. 2. (a) Representation of a percolating system with occupation probability p as a square matrix. (b) Representation of plants of types A and B randomly sown in the cells of the matrix according to a predefined proportion $M = 0.6$.

means that a plant of variety B has been sown. Figure 2 shows an example of the random configuration of the mixture of the two plant varieties represented as a percolating system.

The inoculated cells in this initial configuration are taken in a uniform random way over the matrix with a probability I, which represents the ratio of inoculated cells in the matrix.

Once the cells are inoculated, the pathogen might or might not be propagated to neighboring plants, depending on the pathogen susceptibility χ of each variety of plant. In practice, a plant of type A (B) gets infected and develops the disease if a generated random number is less than χ_A (χ_B); otherwise, the plant remains healthy. If the plant is infected and becomes sick, then its cell value is changed from one to zero. Figure 3 shows an outline of this infection propagation process. The matrix in the upper left corner represents the initial distribution of plants sown with a mixture M, while the matrix on the right shows the result of exposure to the pathogen.

Finally, we take as the production yield for each plant variety the number of plants still alive after the infection has spread. With this method, we simulate the behavior of the plant production yield as a function of the probability p and the mixture M.
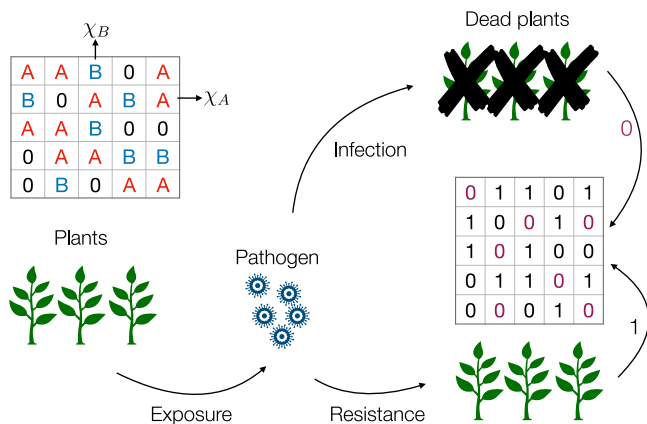

FIG. 3. The pathogen propagation process. The initial configuration (top left) is exposed to the pathogen and each plant has a probability I of being infected. The infected plants are considered as dead and the respective cells in the matrix are marked with a purple zero (right).

III. MATERIAL AND METHODS

A. Substrate preparation

The substrate preparation was carried by mixing peat moss and seived soil (2-mm mesh) in a 1:2 volume-volume mixture. The homogeneous mixture was placed in plastic double bags of 6 kg of high density polyethylene. The bags with the substrate were sterilized in an electric autoclave at 121 °C and 6.8 kg/cm^2 for 30 min for 2 consecutive days.

B. Preparation and treatment of seeds

Three varieties of chili seed were used: "chile de Arbol" from Michoacán, "chile Serrano" from the state of Nayarit, and "chile Poblano" from the state of Puebla. For each one, 100 seeds without deformities were selected. Groups of 100 seeds were selected and weighted for carrying the tests. Each pack of seeds was deflated by adding approximately 20 ml of hydrogen peroxide (9 vol. H_2O_2) in a beaker for a period of 20 min and then rinsed with distilled water for three times and allowed to stand for 2 days immersed in sterile distilled water to promote germination.

C. Preparation of bioassays

For each bioassay, aluminium trays of approximately 3 kg capacity were used. To each tray was added 1.5 kg of sterile substrate, and on it the seed was spread homogeneously and finally covered with 1 kg more of substrate, moistened with enough water, and covered with black bags.

The trays were watered daily with enough water to maintain the humidity until beginning to see the buds of seedlings. The initial growth was observed eight days after sowing. From this moment, it was fertilized every 7 days with 1.9 g/l of the fertilizer blue Nitrofoska.

D. Inoculation of soil with oomycetes

The microorganisms used were taken from the phytopathogenic oomycete strain collection of the Biotechnology Academic Program at the Universidad Politécnica de Puebla. The isolates were reactivated in a selective agar-corn medium added with a mixing of antibiotics (pimaricin, 0.01 g/l; ampicillin, 0.250 g/l; rifampicin, 0.01 g/l).

Each oomycete used was inoculated in the same sterile substrate used for the preparation of the trays. Segments of the growths were inoculated in plastic bags containing 500 g of substrate. The bags were mixed by shaking every 2 days for 3 weeks to ensure the growth of the oomycete throughout the substrate. They were incubated at room temperature. For each inoculated substrate the presence of the respective oomycete was verified by seeding 1 ml of a 1:9 dilution inoculated substrate: water in cornmeal medium-agar added with antibiotics (pimaricin, 0.01 g/l; ampicillin, 0.250 g/l; rifampicin, 0.01 g/l). It was incubated at 27 °C for 5 days.

E. Inoculation of trays

On average, each tray planted contained about 80 seedlings and each of the oomycetes was inoculated into three trays corresponding to the three varieties of chili. The inoculation

TABLE II. Experimental results of the pathogen susceptibilities for different *Capsicum* varieties: "Chile Serrano" (χ_S), "Chile de Arbol" (χ_A), and "Chile Poblano" (χ_P), exposed to several *Phytophthora* isolates.

Oomycete	χ_S	χ_A	χ_P	Kruskal-Wallis test
PcV01	0.60	1.0	0.89	$\Pr < 0.0001$ $A = P$
PcV51	0.46	0.27	0.76	$\Pr < 0.0006$
PcV77	0.64	0.36	0.04	$\Pr < 0.0001$ but $A = P$
PcV90	0.40	0.10	0.19	$\Pr < 0.0002$ all the same
Blank test	0	0	0	

was carried out by adding in the center of each tray 10 g of soil infested by the oomycete corresponding to the treatment. Then it was irrigated with water to favor infestation. Before the inoculation, a census of plants was carried out for each tray.

The fertilization of the plants was stopped at the microorganism inoculation. However, the humidity was maintained at field capacity during the whole time of the test, and 35 days after sowing, live plants were counted in each tray and the survival percentage was calculated.

IV. RESULTS

In this section we show results for the pathogen susceptibility of chili plants of the "Arbol," "Serrano," and "Poblano" varieties exposed to the pathogen oomycete *P. capsici*. We also present the conditions predicted by our model that maximize the production of mixtures of two of these varieties of chili plants when the portion of inoculated cells is 1%, 5%, and 10%.

A. Susceptibility of chili varieties exposed to different *P. capsici* isolates

We obtained the survival rate experimentally by exposing a number of plants to the pathogen and noting the number of alive plants after the period of time mentioned in Sec. III. We denote the survival rate of a plant type exposed to a pathogen (expressed as a percentage) as $\mathcal{P}$, then, the pathogen susceptibility is calculated as

$$\chi = 1 - \frac{\mathcal{P}}{100}. \tag{6}$$

Table II shows the pathogen susceptibility calculated with Eq. (6) for the varieties of "Serrano" (S), "Arbol" (A), and "Poblano" (P) plants of chili exposed to various strains of the pathogen *P. capsici* denoted by PcV and a number to distinguish them from each other.

We actually measured susceptibilities for 20 different strains (including their respective blank tests). These measurements were carried out in a period of approximately 5 months since the procedure described in Sec. III was repeated for all 20 strains in a small green house. The space and time limitation precluded the measurements to be performed more than once. We report susceptibility values for the four strains we consider to be representative for the analysis done in this study. On the other hand, we used Kruskal-Wallis tests to
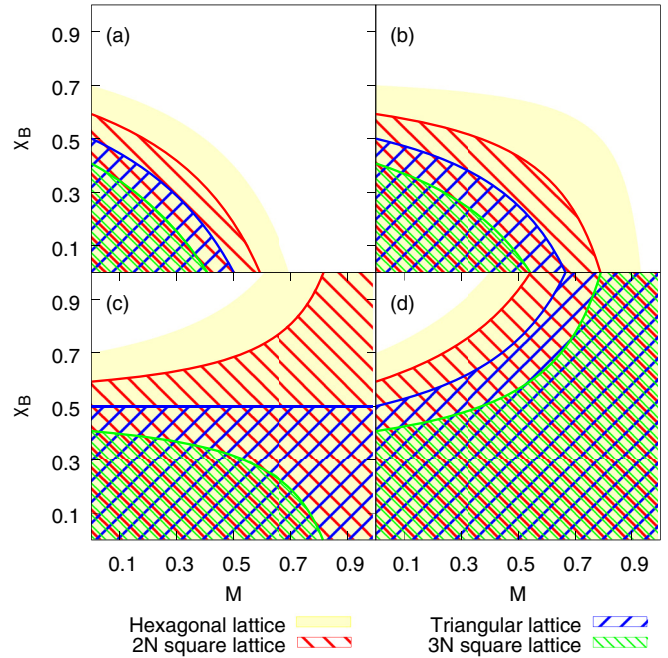

FIG. 4. Examples of conditions for no percolation in regular lattices when the density of inoculated cells is small ($I \to 0$) for values of $\chi_A = 1.00$ (a), 0.75 (b), 0.50 (c), 0.25 (d), when the pathogen propagates over 2N square (red inverse diagonal filled), 3N square (green inverse diagonal filled), triangular (blue diagonal filled), and hexagonal (yellow filled) lattices.

determine that at least two of the compared groups per strain are significantly different whenever the distribution of their data was not a normal distribution. In Table II Pr denotes the probability that a false negative occurred. The small values we obtained mean the three chilis actually have different susceptibilities to the pathogen.

Using the data in Table II, we found the conditions on M and p that optimize the production of the three possible mixtures of two varieties of chili: A-P, A-S, and P-S.

B. Regular lattices

As mentioned in Sec. II A, depending on the values of the pathogen susceptibility of each plant, we can determine the values of M for which the pathogen will only spread on finite clusters, even if all cells are sown. In Fig. 4 we show the combinations of pathogen susceptibility χ_B and mixture M that prevent the formation of the spanning cluster for fixed $\chi_A = 1.00, 0.75, 0.50,$ and 0.25 in different regular lattices in the limit $I \to 0$, corresponding to a single initial inoculation point.

In an analog way, we determined the conditions on M for given values of I that produce no percolation for the pathogen susceptibilities found experimentally. This allowed us to compute the critical mixture M at which we predict the infection will only spread to finite clusters even if all cells are sown, as is shown in Fig. 5. In this context, $M = 0$ ($M = 1$) means only plants with the highest (lowest) susceptibility were sown. Note that the case $M = 1$ can occur as long as one of the plants has a susceptibility small enough to
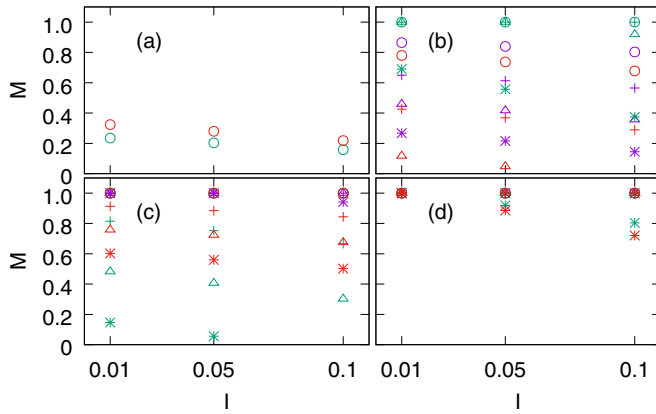
FIG. 5. Conditions for no percolation in 2N (crosses), 3N (stars), triangular (triangles), and hexagonal (circles) lattices of different chili plants mixtures: *A*-*P* (purple), *A*-*S* (green), and *P*-*S* (red) exposed to the strains PcV01 (a), PcV51 (b), PcV77 (c), and PcV90 (d) considering three values of inoculated cells density $I = 0.01$, 0.05, and 0.10.

suppress the pathogen spreading. Such is the case for the PcV90 strain for which the three varieties of chili have small susceptibilities as shown in Fig. 5(d). As it can be seen in Fig. 5, almost all combinations of chili plants in almost all the regular lattices yield $M = 1$. On the other hand, for the cases of strains PcV51, Fig. 5(b), and PcV77, Fig. 5(c), there are several values of the mixture different from 1. In these cases, a more resistant variety of chili must be introduced to avoid the spread of the disease over the most susceptible plant. The most interesting case occurs when plants are exposed to the strain PcV01, Fig. 5(a), since we only found mixing values where the disease does not spread for hexagonal lattices. This singular case is analyzed in Sec. IV C, where we determine conditions for which the production of plants is optimized.

C. Simulation on square lattices

To estimate the production yield as a function of the probability of occupation p and the mixture M, we perform simulations in square matrices of size 100×100. We start with initial values of 0.05 for both p and M. First, we increase

the value of p up to 0.95, in increments of $\Delta p = 0.05$. We then increase the value of M in steps of size $\Delta M = 0.05$ repeating the scan in p for each value of M, up to $M = 0.95$. The simulation was performed 2×10^4 times for each pair of values of p and M, for the three possible chili combinations: *P*-*S*, *A*-*P*, and *S*-*A*, using the pathogen susceptibilities reported in Table II.

In Fig. 6 we show the production yield obtained by computer simulation for the *P*-*S* mixture in the presence of the pathogen PcV01 with different densities of inoculated soil ($I = 0.01$, $I = 0.05$, and $I = 0.1$) in a nearest-neighbor square lattice. The darkest areas indicate the values of density of plants p and mixture M for which the production yield is maximized.

Figure 7 shows level curves of the production yield for different densities of inoculated cells in nearest neighbors (red lines) and next-to-nearest-neighbor (blue lines) square lattices. The production levels were obtained through extrapolation using cubic splines between adjacent points in the p-M plane. Then the level curves of the results obtained by computer simulation were determined. The curves on the graphs in Fig. 7 bound the region where the maximum production yield reaches a certain value, which is indicated by a label on each line.

Finite-size effects on the production yield curves

As is usual in percolation theory some dependence of the observed quantities on the system size is expected: the so-called *finite-size effects* [58–61]. In our case the system size corresponds simply to the matrix size ($L \times L$) which we use in our simulations. To observe these effects we study the behavior of the 35%, 45%, and 55% production level curves for the *P*-*S* mixture shown in Fig. 7(a) as a function of L. Figure 8 shows these curves for $I = 0.01$ in a nearest-neighbor square lattice for different matrix sizes.

It is clear that dependence of the production curves on L is rapidly lost. For occupation probabilities below 0.6 the curves are practically independent of L, in agreement with the fact that the effective probability of the simulated systems is low ($p_{\text{eff}} \leqslant 0.52$ for all M) and therefore the process propagates over finite clusters. In contrast, for larger p values, larger
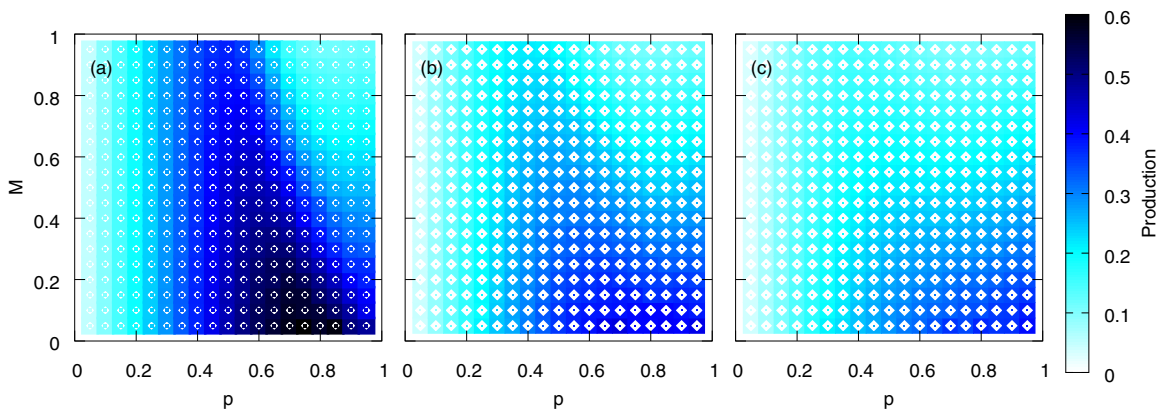

FIG. 6. Simulation results for the production of cells with alive plants after the spreading of the disease on the chili mix *P*-*S* for values of inoculated cells $I = 0.01$ (a), 0.05 (b), and 0.10 (c). Regions in dark represent the higher production yields.
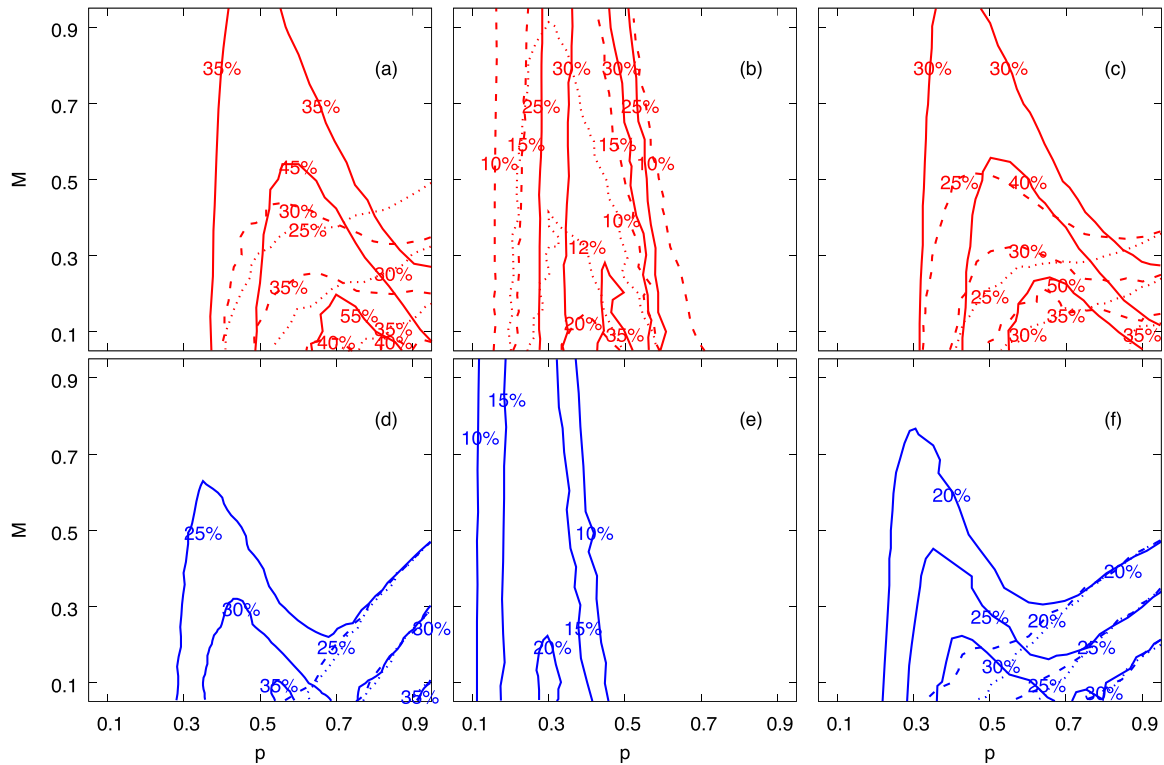
FIG. 7. Level curves for the production yield in terms of the density of plants and the mixture for the three combinations of chili plants at different inoculation densities $I = 0.01$ (solid lines), $I = 0.05$ (dashed lines), and $I = 0.10$ (dotted lines). Top row (red curves) correspond to a nearest-neighbor square lattice for the P-S(a), A-P (b), and S-A (c) mixtures. Bottom row (blue curves) correspond to a next-to-nearest-neighbor square lattice for the P-S (d), A-P (e), and S-A (f) mixtures.

clusters are formed with corresponding larger fluctuations of their probability distribution. Furthermore, the absolute num-

FIG. 8. Finite-size effect on the production yield lines for the P-S mixing exposed to PcV01 with a percentage of inoculated soil $I = 0.01$ in a nearest-neighbors square lattice.

ber of initially inoculated sites grows as IL^2 so the number of inoculated sites is, for example, two orders of magnitude less in a system with $L = 20$ than that of a system with $L = 200$. This means that the number of explored clusters for the propagation of the infection is much limited in small size systems.

V. DISCUSSION

In this paper we proposed a strategy based on percolation theory on regular (triangular, square, and hexagonal) lattices to optimize the production of crops in a plantation. The strategy consists in sowing two varieties of plants with different susceptibilities to a specific pathogen arranged as a percolating system in order to maximize the number of plants that survive an infestation. We assumed that the lattice spacing in the percolation system coincides with the maximum distance that the pathogen can travel before entering a state of dormancy or before dying due to starvation.

We were able to establish a relationship between the percolation threshold of systems with two different probabilities for the occurrence of the propagation process and the parameters of the plantation. Namely the pathogen susceptibilities χ_A and χ_B of each type of plant, the mixture M, the fraction of sites that can initiate infection I, and the percolation threshold of the lattice in which the plants are sown. We also found that, under particular conditions of pathogen susceptibility, there are values of the mixture M for which the disease will only propagate on finite clusters even if all the soil is sown.
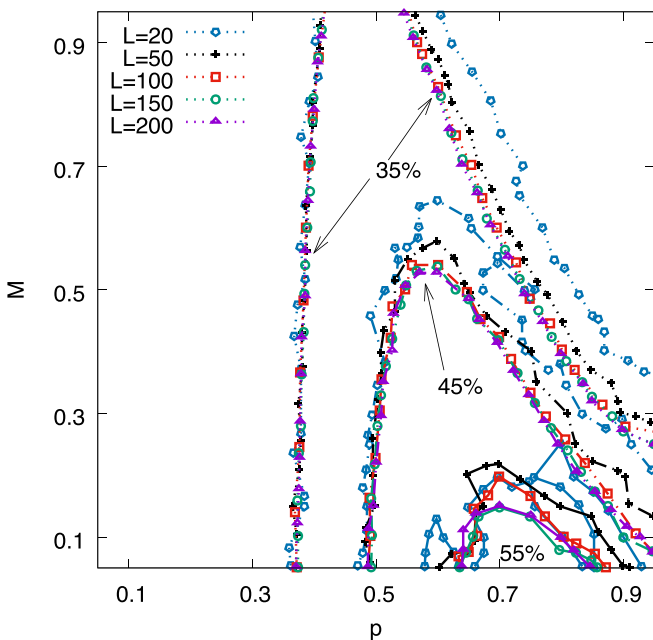
We experimentally measured the pathogen susceptibility to different varieties of the *Phytophtora* pathogen of three chili varieties: "Serrano," "Arbol," and "Poblano" which are of commercial value in Mexico. We found that for the pathogens catalogued as PcV51, PcV77, and PcV90, there are values of the mixture M for which the infection will only spread on finite clusters, independently of the regular lattice that is considered. On the other hand, we found that the mortality rate of the plants in presence of PcV01 is relatively high, so it is not possible to find mixing values for which the infection propagates on finite clusters. For this particular case, we determined by computer simulation the production yield of the three possible pairs of plants for three different percentages of inoculated soil $I = 0.01, 0.05,$ and 0.10. We found the production yield is highly sensitive to the amount of soil inoculated and there is a considerable difference in production yield for the extreme values of I. In addition, the production yield for the next-to-nearest-neighbor lattice is lower than that for the nearest-neighbor lattice due to the fact that in the 3N square lattice, the number of coordination is larger than in the 2N square lattice, which means that the pathogen has more options to spread.

In the most drastic case of pathogen susceptibility, the "Arbol" variety was measured to have $\chi_A = 1$, which means the infection will spread over all the plants regardless of the percentage of inoculated land when all the soil is sown. However, when mixed with the "Serrano" variety ($\chi_S = 0.6$) on a nearest-neighbor square lattice, we found total production level curves of 50%, 35%, and 30% of the total cells for inoculated soil levels of $I = 0.01, 0.05,$ and 0.10, respectively. On the other hand, on a next-to-nearest-neighbor square lattice we found production level curves around 30% regardless of the fraction of the soil inoculated. These results show that the production of "Arbol" could be improved if sown in combination with a second variety of chili plant.

We compared the predictions of our model to the simulated production yield for a crop with a mixing of two chilis sowed in alternate rows of the lattice. That is sowing one of the varieties in all sites of a row and filling the next row with the other type of chili. We found the production yield for each of the three combinations of chilis does not depend on the coordination number of the lattice nor on the fraction of soil initially inoculated. For these varieties with pathogen susceptibilities close to 1 the production yield is given by $1 - (\chi_A + \chi_B)/2$. For example, in the S-A mixing exposed to PcV01, on the average, half of the initially inoculated plants will be of the variety A and then the corresponding rows rows will be completely lost since $\chi_A = 1$. Consequently, the rows with variety S will in fact be exposed to the pathogen and only the resistant plants will survive. At the same time, the infected plants of variety S will continue propagating the pathogen to the next row and so on. At the end of the propagation process, only resistant plants of the variety S will be alive, which corresponds to 20% of all cells (since the mixing proportion is 50% and $\chi_S = 0.6$). And the pathogen will spread over all the lattice. On the other hand, using our model, there is a production yield curve corresponding to 50% ($\sim$10% of variety A+ $\sim$ 40% of variety S).

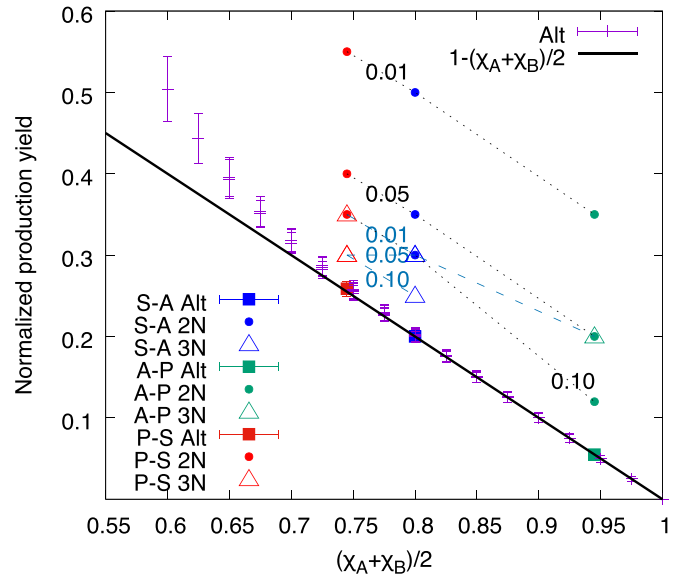In Fig. 9 we show the yield production for the alternate rows strategy and the maximum percentage observed for the

FIG. 9. Comparison of the production yield between the alternate rows sowing (filled squares) and the percolation strategy for the P-S (red), A-P (green), and S-A (blue) mixings, for plants exposed to PcV01. Simulations of the percolation strategy in 2N (filled circles) and 3N (triangles) lattices for different fractions of inoculated soil ($I = 0.01, 0.05, 0.1$) are shown. Production yield of systems sowed in alternate rows with different combinations of pathogen susceptibilities (purple points) agree with $1 - (\chi_A + \chi_B)/2$ (black curve) for high susceptibilities values.

percolation strategy in 2N and 3N square lattices. Simulations of alternate rows sowing for other combinations of pathogen susceptibilities were performed (see the purple points in Fig. 9). Note that for those systems where the pathogen is high for both plant varieties, the normalized production yield is well fitted by $1 - (\chi_A + \chi_B)/2$. Finally, the percolation strategy presented here predicts a better production yield than the alternate rows sowing strategy, even in those systems where the pathogen can reach next to nearest neighbors in the square lattice for the three analyzed fractions of inoculated soil.

VI. CONCLUSIONS AND PERSPECTIVES

In this work, we have presented and implemented a model based on percolation theory to avoid the spreading process of a pathogen with the capability of movement (by flagella) through plants with high susceptibility by the sowing of a plant mixture with less pathogen susceptibility. We have determined the percolation threshold and the no percolation condition for these systems considering the following variables: density of cells sown, pathogen susceptibilities, the portion of plant mix, and the percentage of inoculated soil. This strategy can be applied in a whole variety of cases. Also, for those systems where it is not possible to determine the no percolation conditions, we presented the corresponding Monte Carlo simulation. The main result of this approach is the possibility to raise the production yield of the plant with high pathogen susceptibility, even when the yield production is close to zero under traditional sowing conditions.

The strategy presented here could help farmers to select the type of plants that would give the best production yield on their land without applying any pesticides or chemical products. The required parameters to predict the production yield for a given mixture of plants are just the percentage of soil initially inoculated and the pathogen susceptibilities of the plants involved. One has to consider that applying this model to a real-life situation, farmers should now be interested in the physical and chemical properties of harmful microorganisms that inhabit their land and in the response of the desired plants to sow in the presence of those pathogens. These properties would enable them to determine the sowing conditions that would optimize the harvest.

Since the model allows for available cells, a third plant variety can be added in the empty spaces. This would clearly permit farmers to better exploit their agronomic resources with the only restriction of choosing a more resistant variety of plant. This proposal is in agreement with polyculture, which is promoted as a way for sustainable use of soils.

The model could be straightforwardly extended to assess the effect of additional variables of the pathogen dynamics on the propagation of the disease, giving a more accurate prediction of the production yield. For example, reinfection and recovery of some plants were observed on our experiments. The plant reinfection lapse and the recovery time could be measured and implemented in our model using an SIR model approach.

Finally, some other types of variables might also be included, such as the care provided by the farmer or the possibility of having more than one type of pathogen in the field. This occurs, for example, with *P. capsici*, whose subvarieties can all be found in the same parcel.

ACKNOWLEDGMENTS

[1] S. R. Broadbent and J. M. Hammersley, Math. Proc. Cambridge Philos. Soc. **53**, 629 (1957).

[2] M. Sahini and M. Sahimi, *Applications of Percolation Theory* (CRC Press, London, 2014).

[3] S. Kirkpatrick, Rev. Mod. Phys. **45**, 574 (1973).

[4] D. Stauffer and A. Aharony, *Introduction To Percolation Theory,* revised 2nd ed. (CRC Press, Boca Raton, FL, 2014).

[5] G. Grimmett, *Percolation*, Grundlehren der mathematischen Wissenschaften (Springer, Berlin, 2013).

[6] A. A. Saberi, Phys. Rep. **578**, 1 (2015).

[7] D. Stauffer, Phys. Rep. **54**, 1 (1979).

[8] D. Stauffer, A. Coniglio, and M. Adam, in *Polymer Networks*, edited by K. Dušek (Springer, Berlin, 1982), pp. 103–158.

[9] P. E. Seiden and L. S. Schulman, Adv. Phys. **39**, 1 (1990).

[10] A. Klypin and S. F. Shandarin, Astrophys. J. **413**, 48 (1993).

[11] L. S. Schulman and P. E. Seiden, Science **233**, 425 (1986).

[12] H. E. Stanley, J. Phys. A: Math. Gen. **12**, L329 (1979).

[13] C. K. Hu, J. Phys. A: Math. Gen. **16**, L321 (1983).

[14] G. Wagner, A. Birovljev, P. Meakin, J. Feder, and T. Jøssang, Phys. Rev. E **55**, 7015 (1997).

[15] I. Kantorovich and E. Bar-Ziv, Combust. Flame **113**, 532 (1998).

[16] X. Campi, H. Krivine, N. Sator, and E. Plagnol, Eur. Phys. J. D **11**, 233 (2000).

[17] M. Sahimi and D. Stauffer, Chem. Eng. Sci. **46**, 2225 (1991).

[18] B. Ghanbarian, H. Daigle, A. G. Hunt, R. P. Ewing, and M. Sahimi, J. Geophys. Res.: Solid Earth **120**, 182 (2014).

[19] M. Sahimi, Physica A **186**, 160 (1992).

[20] B. K. Chakrabarti, Rep. Adv. Phys. Sci. **01**, 1750013 (2017).

[21] A. Sakhaee-Pour and A. Agrawal, J. Pet. Sci. Eng. **160**, 152 (2018).

[22] T. Ohtsuki and T. Keyes, J. Phys. A: Math. Gen. **19**, L281 (1986).

[23] T. Beer and I. Enting, Math. Comput. Model. **13**, 77 (1990).

[24] B. Drossel and F. Schwabl, Phys. Rev. Lett. **69**, 1629 (1992).

[25] F. Taubert, R. Fischer, J. Groeneveld, S. Lehmann, M. S. Müller, E. Rödig, T. Wiegand, and A. Huth, Nature **554**, 519 (2018).

[26] G. Baym, Physica A **96**, 131 (1979).

[27] X. Campi, J. Phys. A: Math. Gen. **19**, L917 (1986).

[28] J. E. Ramírez, A. Fernández Téllez, and I. Bautista, Physica A. **488**, 8 (2017).

[29] D. S. Callaway, M. E. J. Newman, S. H. Strogatz, and D. J. Watts, Phys. Rev. Lett. **85**, 5468 (2000).

[30] M. E. J. Newman and D. J. Watts, Phys. Rev. E **60**, 7332 (1999).

[31] C. Moore and M. E. J. Newman, Phys. Rev. E **61**, 5678 (2000).

[32] M. E. J. Newman, Phys. Rev. E **66**, 016128 (2002).

[33] M. E. J. Newman, Phys. Rev. Lett. **89**, 208701 (2002).

[34] L. Meyers, Bull. Am. Math. Soc. **44**, 63 (2007).

[35] E. B. Postnikov and I. M. Sokolov, Math. Biosci. **208**, 205 (2007).

[36] J. C. Miller, Phys. Rev. E **80**, 020901 (2009).

[37] E. Massaro and F. Bagnoli, Phys. Rev. E **90**, 052817 (2014).

[38] B. Dybiec, A. Kleczkowski, and C. A. Gilligan, Phys. Rev. E **70**, 066145 (2004).

[39] M. W. Shaw, Annu. Rev. Phytopathol. **32**, 523 (1994).

[40] D. J. Bailey, W. Otten, and C. A. Gilligan, New Phytol. **146**, 535 (2000).

[41] G. J. Gibson, W. Otten, J. A. N. Filipe, A. Cook, G. Marion, and C. A. Gilligan, Stat. Comput. **16**, 391 (2006).

[42] W. Otten and C. A. Gilligan, Eur. J. Soil Sci. **57**, 26 (2006).

[43] C. C. Mundt and K. E. Sackett, Ecosphere **3**, art24 (2012).

[44] T. Reglinski, M. Spiers, J. Taylor, and M. Dick, New Zealand J. Forestry **54**, 16 (2010).

[45] M. Thines and S. Kamoun, Curr. Opin. Plant Biol. **13**, 427 (2010).

[46] K. H. Lamour, R. Stam, J. Jupe, and E. Huitema, Mol. Plant Pathol. **13**, 329 (2011).

[47] P. van West, A. A. Appiah, and N. A. Gow, Physiol. Mol. Plant Pathol. **62**, 99 (2003), root Diseases.

[48] M. W. Dick, in *Systematics and Evolution*, edited by D. J. McLaughlin, E. G. McLaughlin, and P. A. Lemke (Springer, Berlin, 2001), pp. 39–72.

[49] D. C. Erwin and O. K. Ribeiro, *Phytophthora Diseases Worldwide* (American Phytopathological Society Press, Minnesota, 1996).

[50] See Supplemental Material at http://link.aps.org/supplemental/10.1103/PhysRevE.98.062409 for a microscope video showing the slight movements of *Phytophthora*.

[51] E. A. Bernhardt and R. G. Grogan, Phytopathology (USA) **72**, 507 (1982).

[52] A. R. Hardham, Mol. Plant Pathol. **6**, 589 (2005).

[53] B. Feng, P. Li, H. Wang, and X. Zhang, Microb. Pathog. **49**, 23 (2010).

[54] P. Li, B. Feng, H. Wang, P. W. Tooley, and X. Zhang, J. Basic Microbiol. **51**, 61 (2011).

[55] R. N. Trigiano, *Plant Pathology Concepts and Laboratory Exercises* (CRC Press, Boca Raton, FL, 2007).

[56] H. V. Silva-Rojas, S. P. Fernández-Pavia, C. Góngora-Canul, B. C. Macías-López, and G. D. Ávila-Quezada, Rev. Mex. Fitopatol. **27**, 134 (2009).

[57] G. Gilardi, M. Baudino, M. Moizio, M. Pugliese, A. Garibaldi, and M. Gullino, Crop Protection **53**, 13 (2013).

[58] C. D. Lorenz and R. M. Ziff, Phys. Rev. E **57**, 230 (1998).

[59] J. Schmelzer, S. A. Brown, A. Wurl, M. Hyslop, and R. J. Blaikie, Phys. Rev. Lett. **88**, 226802 (2002).

[60] R. Kenna and B. Berche, J. Phys. A: Math. Theor. **50**, 235001 (2017).

[61] B. Roy and S. Santra, Physica A **492**, 969 (2018).